A STUDY OF OPTICAL TRANSMISSIVITY AND OPTICAL PHASE RETARDATION MEASUREMENT BY USING A FIBER LOOP MIRROR ARCHITECTURE

KANITHA KATANYUKUNANON

A THESIS SUBMITTED IN PARTIAL FULFILLMENT
OF THE REQUIREMENTS FOR
THE DEGREE OF MASTER OF SCIENCE (PHYSICS)
FACULTY OF GRADUATE STUDIES
MAHIDOL UNIVERSITY
2007

COPYRIGHT OF MAHIDOL UNIVERSITY

Copyright by Mahidol University

Thesis
Entitled

A STUDY OF OPTICAL TRANSMISSIVITY AND OPTICAL PHASE RETARDATION MEASUREMENT BY USING A FIBER LOOP MIRROR ARCHITECTURE

Kanitha Katanyukunanon

Ms. Kanitha Katanyukunanon
Candidate

Assist. Prof. Toemsak Srikhirin, Ph.D.
Major-Advisor

Sarun Sumriddetchkajorn

Mr. Sarun Sumriddetchkajorn, Ph.D.
Co-Advisor

B. Mahaisavariya

Prof. Banchong Mahaisavariya, M.D.
Dean
Faculty of Graduate Studies

Assist. Prof. Wannapong Triampo, Ph.D.
Chair
Master of Science Programme in Physics
Faculty of Science

Copyright by Mahidol University

Thesis
Entitled

A STUDY OF OPTICAL TRANSMISSIVITY AND OPTICAL PHASE RETARDATION MEASUREMENT BY USING A FIBER LOOP MIRROR ARCHITECTURE

was submitted to the Faculty of Graduate Studies, Mahidol University
for the degree of Master of Science (Physics)
on
October 4, 2007

Kanitha Katanyukunanon
Ms. Kanitha Katanyukunanon
Candidate

R Chitaree
Assist. Prof. Ratchapak Chitaree,
Ph.D.
Member

Prathan Buranasiri
Mr. Prathan Buranasiri,
Ph.D.
Chair

Sarun Sumriddetchkajorn
Mr. Sarun Sumriddetchkajorn,
Ph.D.
Member

Assist. Prof. Toemsak Srikhirin,
Ph.D.
Member

B. Mahaisavariya
Prof. Banchong Mahaisavariya, M.D.
Dean
Faculty of Graduate Studies
Mahidol University

Amaret Bhumiratana
Prof. Amaret Bhumiratana,
Ph.D.
Dean
Faculty of Science
Mahidol University

Copyright by Mahidol University

ACKNOWLEDGEMENTS

This thesis can be succeeded by the extensive support and assistance from my major advisor, Assist. Prof. Dr. Toemsak Srikhirin and my co-advisor, Dr. Sarun Sumriddetchkajorn. I am grateful to them for their valuable advice and guidance on this research.

I wish to thank Dr. Prathan Buranasiri and Assist. Prof. Dr. Ratchapak Chitaree for his helpful comments and evaluating this thesis.

I wish to thank the Thailand Graduate Institute of Science and Technology (TGIST), grant number: TGIST 01-48-008 for their financial support.

I would also like to express my gratitude to everyone at the National Electronics and Computer Technology Center (NECTEC)'s Photonics Technology Laboratory who helped and taught me.

I greatly appreciate all my friends and staff at the Capability Building Unit in the Nanoscience and Nanotechnology at Mahidol University for their kind support and cheerfulness.

Finally, I would like to express my sincere gratitude to my family for their encouragement and love.

Kanitha Katanyukunanon

Copyright by Mahidol University

A STUDY OF OPTICAL TRANSMISSIVITY AND OPTICAL PHASE RETARDATION MEASUREMENT BY USING A FIBER LOOP MIRROR ARCHITECTURE

KANITHA KATANYUKUNANON 4836486 SCPY/M

M.Sc. (PHYSICS)

THESIS ADVISORS : TOEMSAK SRIKHIRIN, Ph.D. (POLYMER SCIENCE AND ENGINEERING), SARUN SUMRIDDETCHKAJORN, Ph.D. (OPTICAL SCIENCE AND ENGINEERING)

ABSTRACT

This thesis proposes and experimentally demonstrates a fiber-connectorized optical system that can be used to study both the optical transmissivity and optical phase retardation of the material. The key idea comes from the inherent advantages of the fiber loop mirror (FLM) which simply consists of a 2×2 fiber-optic coupler and a polarization controller. The FLM has been found to be a more appropriate choice once its two output ports are analyzed simultaneously for the implementation of an optical sensing system that can examine at least two interest parameters and requires less precise free-space optical alignment. In this thesis, the FLM operation which is based on the interference of the two counter-propagating optical beams as well as the optical phase retardation induced inside the FLM was studied. In this experiment, it was decided to vary the FLM transmissivity and reflectivity by simply adjusting the polarization controller in the loop. As a result, it could be optimized the maximum transmission of the FLM for analyzing the optical transmissivity of the desired test sample. In addition, using the same setup it was proposed to eliminate the effect of optical losses from the test sample and the FLM itself in measuring the optical phase retardation of the test sample via analyzing the ratio of the optical powers from both transmission and reflection ports of the FLM. The experimental proof of this concept using three known zero-order waveplates as test samples shows promising results which agree very well with the theoretical analysis proposed in this thesis.

KEY WORDS: FIBER LOOP MIRROR ARCHITECTURE / OPTICAL TRANSMISSIVITY / OPTICAL PHASE RETARDATION

35 P.

Copyright by Mahidol University

การศึกษาการวัดค่าการส่งผ่านและค่าความต่างเฟสของแสงของวัตถุในสถาปัตยกรรมกระจกสะท้อนแบบไฟเบอร์ลูป

(A STUDY OF OPTICAL TRANSMISSIVITY AND OPTICAL PHASE RETARDATION MEASUREMENT BY USING A FIBER LOOP MIRROR ARCHITECTURE)

ขนิษฐา กตัญญุคุณานนท์ 4836486 SCPY/M

วท.ม. (ฟิสิกส์)

คณะกรรมการควบคุมวิทยานิพนธ์ : เติมศักดิ์ ศรีคิรินทร์, Ph.D. (Polymer Science and Engineering), ศรัณย์ สัมฤทธิ์เดชขจร, Ph.D. (Optical Science and Engineering)

บทคัดย่อ

วิทยานิพนธ์นี้ แสดงให้เห็นถึงระบบเชิงแสงที่เชื่อมต่อกันด้วยเส้นใยแก้วนำแสง ซึ่งสามารถใช้ศึกษาได้ทั้งค่าการส่งผ่านของแสงและค่าความต่างเฟสของแสงของวัตถุ โดยได้แนวความคิดมาจากข้อได้เปรียบของโครงสร้างกระจกสะท้อนแบบไฟเบอร์ลูปที่ประกอบด้วย 2×2 ไฟเบอร์ออปติกคัปเปลอร์และอุปกรณ์ควบคุมโพลาไรเซชั่นของแสง ซึ่งโครงสร้างดังกล่าวนี้เป็นหนึ่งทางเลือกที่มีความเหมาะสมสำหรับสร้างเป็นอุปกรณ์ตรวจวัดเชิงแสงที่สามารถตรวจวัดคุณสมบัติทางแสงที่น่าสนใจได้อย่างน้อยสองคุณสมบัติอีกทั้งยังมีช่องว่างที่ต้องมีการจัดแสงให้อยู่ในแนวเดียวกันเล็กน้อย วิทยานิพนธ์เล่มนี้ได้ศึกษาถึงหลักการทำงานของกระจกสะท้อนแบบไฟเบอร์ลูปซึ่งอยู่บนพื้นฐานของการแทรกสอดกันของแสงที่เคลื่อนที่ในทิศทางตรงข้ามกันพร้อมกับก่อให้เกิดค่าความต่างเฟสของแสงขึ้นภายในกระจกสะท้อนแบบไฟเบอร์ลูป จากการทดลอง เราเลือกที่จะปรับเปลี่ยนค่าการส่งผ่านและค่าสะท้อนกลับของแสงในกระจกสะท้อนแบบไฟเบอร์ลูปโดยการปรับอุปกรณ์ควบคุมโพลาไรเซชั่นของแสงที่อยู่ภายในลูป ซึ่งผลดังกล่าวสามารถทำให้ได้ค่าการส่งผ่านของแสงที่มีค่ามากที่สุดเพื่อใช้ในการวิเคราะห์ค่าการส่งผ่านของแสงของตัวอย่างที่ต้องการทดสอบ นอกจากนี้การใช้โครงสร้างเดียวกันนี้ เราเสนอที่จะกำจัดผลกระทบของค่าการสูญเสียทางแสงจากตัวอย่างทดสอบและจากตัวโครงสร้างกระจกสะท้อนแบบไฟเบอร์ลูปเอง ในการวัดค่าความต่างเฟสของแสงของตัวอย่างทดสอบด้วยการวิเคราะห์อัตราส่วนของกำลังของแสงทั้งจากพอร์ททะลุผ่านและสะท้อนกลับของโครงสร้างกระจกสะท้อนแบบไฟเบอร์ลูป จากการทดลองกับตัวหน่วงเฟสพิสูจน์ได้ว่าค่าการส่งผ่านของแสงและค่าความต่างเฟสของแสงที่ได้จากตัวอย่างนั้นมีความสอดคล้องกับค่าทางทฤษฎีเป็นอย่างดี

35 หน้า

Copyright by Mahidol University

CONTENTS

	Page
ACKNOWLEDGEMENTS	iii
ABSTRACT (English)	iv
ABSTRACT (Thai)	v
LIST OF FIGURES	viii
CHAPTER	
I INTRODUCTION	1
II FIBER LOOP MIRROR (FLM)	5
2.1 FLM structure	5
2.2 Operating principle	6
2.3 Applications	9
III FLM-BASED ARCHITECTURE	11
3.1 Our proposed architecture	11
3.1.1 Optical transmissivity measurement	12
3.1.2 Optical phase retardation measurement	13
3.2 Experimental setup	16
3.2.1 Fiber-optic circulator	18
3.2.2 Fiber-optic coupler	18
3.2.3 Fiber-optic collimator	19
3.2.4 Polarization controller (PC)	19

Copyright by Mahidol University

CONTENTS (cont.)

	Page
IV RESULT AND DISCUSSION	21
4.1 Optical isolation study	21
4.2 Optical loss study	22
4.3 Polarization dependent loss study	23
4.4 Optical transmissivity study	23
4.5 Optical phase retardation study	25
V CONCLUSIONS	27
REFERENCES	29
BIOGRAPHY	35

Copyright by Mahidol University

LIST OF FIGURES

Figure	Page
1.1 A typical optical spectrometer	1
1.2 A polarimeter	2
2.1 A fiber loop mirror structure	6
2.2 Propagation of p-polarized optical beam around the FLM when the FLM acts as a full waveplate	7
2.3 Propagation of p-polarized optical beam around the FLM when the FLM acts as a half waveplate oriented at 45° with respect to the y axis	7
3.1 Our proposed FLM-based optical phase retardation and optical transmissivity measurement architecture	11
3.2 Calculated normalized optical power ratio PR_2 as a function of coupler splitting ratio and optical phase retardation	14
3.3 Calculated normalized optical power ratio PR_2 versus waveplate orientation angle	15
3.4 (a) Schematic illustration of our experimental setup and	16
(b) photograph of our experimental setup taken at the FLM section. SMF: Single mode optical fiber	17
3.5 Our zero-order waveplates: WP1, WP2, and WP3, respectively	17
3.6 Fiber-optic circulator	18
3.7 2×2 Fiber-optic coupler	18
3.8 Fiber-optic collimator	19
3.9 Polarization controller	19
3.10 Squeezing fiber optic	20
4.1 Measured optical isolation at the port P_2 when the FLM is set to operate only at 1550 nm wavelength	21

Copyright by Mahidol University

LIST OF FIGURES (cont.)

Figure	Page
4.2 Measured optical isolation at the port P_2 when the FLM is optimized to operate at any desired wavelength	22
4.3 Measured optical transmissivity versus operating wavelength for WP1 in (a) an optical spectrometer and (b) our FLM-based structures	23
4.4 Measured optical transmissivity versus operating wavelength for WP2 in (a) an optical spectrometer and (b) our FLM-based structures	24
4.5 Measured optical transmissivity versus operating wavelength for WP3 in (a) an optical spectrometer and (b) our FLM-based structures	24
4.6 Measured normalized optical power ratio versus waveplate orientation angle for (a) WP1, (b) WP2, and (c) WP3	25
4.7 Measured optical phase retardation versus test wavelength for (a) WP1, (b) WP2, and (c) WP3	26

Copyright by Mahidol University

CHAPTER I
INTRODUCTION

A variety of optical sensing structures has been proposed and demonstrated for measuring some optical properties of materials. For example, an optical absorption coefficient (α) can be determined by using an optical spectrometer [1]. Its basic relies on the use of the absorption, emission, or scattering of electromagnetic radiation by atoms or molecules to qualitatively or quantitatively study the atoms or molecules. An optical spectrometer structure consists of a broadband light source, a tunable filter, a sample to be investigated, and a photodetector (PD) as shown in Fig. 1.1.

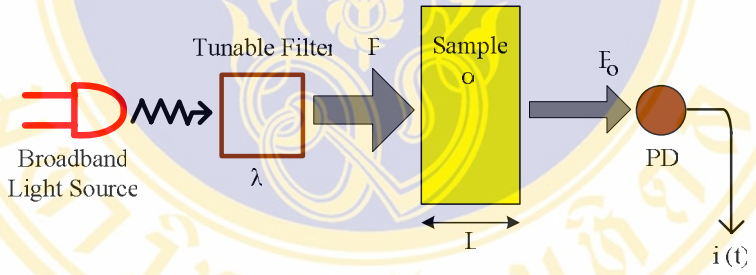

Figure 1.1 A typical optical spectrometer.

When the optical beam having an optical power of P_i passes through the sample, the output optical power (P_o) can be expressed as [2]

$$P_o = P_i e^{-\alpha L}. \tag{1.1}$$

Here, L is the propagating distance of the optical beam inside the sample.

Eqn (1.1) can also be rewritten in terms of absorbance (A) as

$$\ln \frac{P_o}{P_i} = -\alpha L,$$

Copyright by Mahidol University

$$-\log\frac{P_o}{P_i}=\frac{\alpha}{2.303}L,$$

$$A=\log\frac{P_i}{P_o}. \tag{1.2}$$

Based on Eqns(1.1) and (1.2), the absorption coefficient of the sample can be easily determined. The optical power (P_o) emerging from the test material is compared to the incident optical beam power (P_i), also called the optical transmissivity. Increasing L can also improve the sensitivity of the system but it affects the dimensions of the system.

Apart from the absorption coefficient of the material, another interesting optical parameter of the material is its birefringence (Δn) which tells us how different states of polarized lights refract into the material and suffer different phase delay. It is sometimes mentioned as optical phase retardation (Δϕ). In this case, another instrument such as a polarimeter is needed. A polarimeter is an optical instrument used for determining the polarization state of a light beam or the polarization-altering properties of a sample [3]. A most sensitive polarimeter is based on an interferometric effect and polarization modulation [4] while more simple approaches are based on arrangements of polarising filters or waveplates. Fig 1.2 shows an example of a simple polarimeter where the test sample is positioned between two known phase retardation plates ϕ_1 and ϕ_2. There are also two polarizers in front of and behind the first and the second phase retarders, respectively. Both phase retardation plates can be rotated at θ_1 and θ_2, respectively.

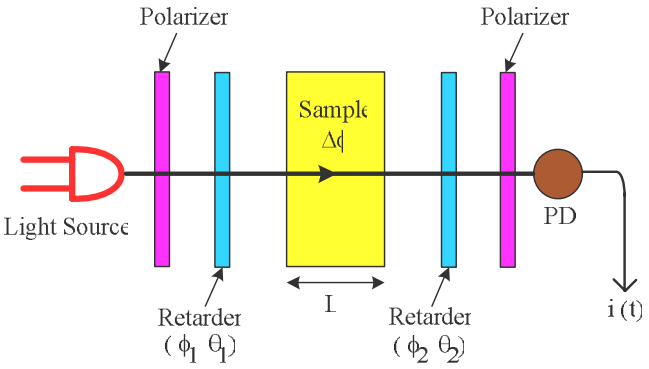

Figure 1.2 A polarimeter.

Copyright by Mahidol University

Knowing ϕ_1, ϕ_2, θ_1 and θ_2, $\Delta\phi$ The normalized intensity on the detector can be computed as [5]

$$I(\theta_1,\theta_2)=(1,0,0,0)PL(\theta=0)WP(\phi_1,\theta_1)M\,WP(\phi_2,\theta_2)\,PL(\theta=0)(1,0,0,0)^t, \quad (1.3)$$

where (1,0,0,0) is the Stokes vector sensed by the detector, PLs are Mueller matrices of fixed linear polarizers behind the light source and in front of the PD, respectively. $WP(\theta_1,\phi_1)$ is the Mueller matrix of the first rotating waveplate while $WP(\theta_2,\phi_2)$ is the Mueller matrix of the second rotating waveplate. ϕ_i and θ_i $(i=1,2)$ are the optical phase retardation and the orientation angle of the waveplate i^{th}, respectively. M is the Mueller matrix of the sample. The superscript t denotes the transpose. The ideal Mueller matrices of a polarizer and a linear retarder are given as

$$PL(\theta)=\frac{1}{2}R(-\theta)\begin{bmatrix}1&1&0&0\\1&1&0&0\\0&0&0&0\\0&0&0&0\end{bmatrix}R(\theta), \quad (1.4)$$

and

$$WP(\phi,\theta)=R(-\theta)\begin{bmatrix}1&0&0&0\\0&1&0&0\\0&0&\cos\phi&\sin\phi\\0&0&-\sin\phi&\cos\phi\end{bmatrix}R(\theta), \quad (1.5)$$

with the matrix of coordinate rotation

$$R(\theta)=\begin{bmatrix}1&0&0&0\\0&\cos 2\theta&\sin 2\theta&0\\0&-\sin 2\theta&\cos 2\theta&0\\0&0&0&1\end{bmatrix}. \quad (1.6)$$

Copyright by Mahidol University

From Eqn(1.3) to Eqn(1.6), it is clear that the optical phase retardation of the sample can be determined by placing a desired test sample between two suitably defined waveplates and then rotating each waveplate independently. Consequently, the level of the output intensity tells us how much the optical phase retardation is.

Based on the structures and the operations of the above optical sensing systems, it is obvious that only one equipment can handle in measuring only one interesting optical parameter. In addition, these instruments are designed and implemented in a free-space architecture and therefore a precise free-space optical alignment is a very important issue. Furthermore, from the optical phase retardation measurement issue, the polarimeter has a complicated optical structure and its analytical procedure is very complex. Hence, it would be desirable to have a fiber-based optical instrument in which more than one parameters (e.g., both optical transmissivity and optical phase retardation) can be investigated under simple analytical models.

In this thesis, we propose to eliminate the need of careful free-space optical adjustment through the use of a fiber loop mirror (FLM) structure. Based on the basic operation of the FLM, we will also show theoretically and experimentally how the FLM can be used to analyze both the optical transmissivity and the optical phase retardation of the test sample in a more convenient way.

Copyright by Mahidol University

CHAPTER II
FIBER LOOP MIRROR (FLM)

Today most deployed components in optical communications such as couplers, optical attenuators, and polarizers are fiber-based devices that provide compactness and compatibility with fiber embedded systems. These components can also be easily connected to each other using either the fiber fusion splicing technique or fiber connectors in order to form a fiber-connectorized sensing system for measuring the optical transmissivity and the optical phase retardation of the sample.

One of the promising fiber-based optical sensing architectures is a fiber loop mirror (FLM) [6]. Since its invention in 1988 based on the Sagnac effect that was previously discovered by Georges Sagnac more than 90 years ago, it has been proposed and experimentally demonstrated for several applications. In this chapter, we show how the FLM can be easily formed. Its basic operation and applications will also be included.

2.1 FLM Structure

An FLM consists of an optical fiber loop formed between the two output ports of a 2×2 fiber-optic coupler as shown in Fig. 2.1. The input light can be transmitted through (i.e., P_2) or retroreflected from (i.e., P_1) the fiber loop, depending on the nature of the optical interference between the clockwise and counterclockwise propagating electric fields inside the fiber loop.

Copyright by Mahidol University

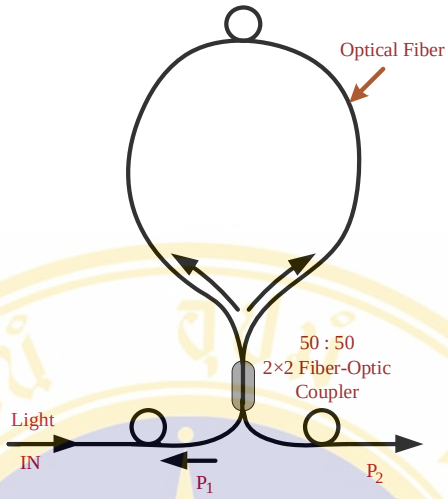

Figure 2.1 A fiber loop mirror structure.

2.2 Operating principle

In the FLM, the input light is reflected from and transmitted through the FLM by the optical interference between two electric fields traveling around the loop in the opposite direction. To understand the operation of the FLM, we can consider feeding a p-polarized optical beam to the port A of the FLM as shown in Fig. 2.2. When the input polarized optical beam reaches the 2×2 fiber-optic coupler having a coupling coefficient (K) of 0.5, it is split equally into two counter-propagating optical beams. In this case, the anticlockwise light coupled from the port 1 to the port 4 of the 2×2 fiber-optic coupler has an additional $\pi/2$ phase shift from the coupler due to the coupling effect. Another optical beam is sent to the port 3 of the 2×2 fiber-optic coupler without affecting its phase. Due to the present of bend, twist, and stress in the optical fiber, the fiber loop inside the FLM can function as a waveplate. Hence, if the fiber loop acts as a full waveplate, two counter-propagating optical beams inside the fiber loop are still p-polarized as shown in Fig. 2.2. In this case, the polarization directions of clockwise and counterclockwise optical beams are pointing out of and in the loop, respectively. After these two counter propagating optical beams travel around the loop, they meet each other again at the 2×2 fiber-optic coupler and the optical interference occurs. At the port A, there are the two optical beams. One is the counterclockwise optical beam that travels directly from the port 3 to the port 1 of the 2×2 fiber-optic coupler. The clockwise optical beam also goes from the port 4 to the

Copyright by Mahidol University

port 1 of the 2×2 fiber-optic coupler via coupling effect. These two optical beams have the same phase shift and their polarization vectors are also in the same direction (i.e., +x axis), thus inducing a constructive interference. In this case, light comes out at the port A. On the other hand, although these two optical beams at the port B are polarized in the x direction, they have a π-phase difference. Hence, a destructive interference occurs and no light comes out at the port B.

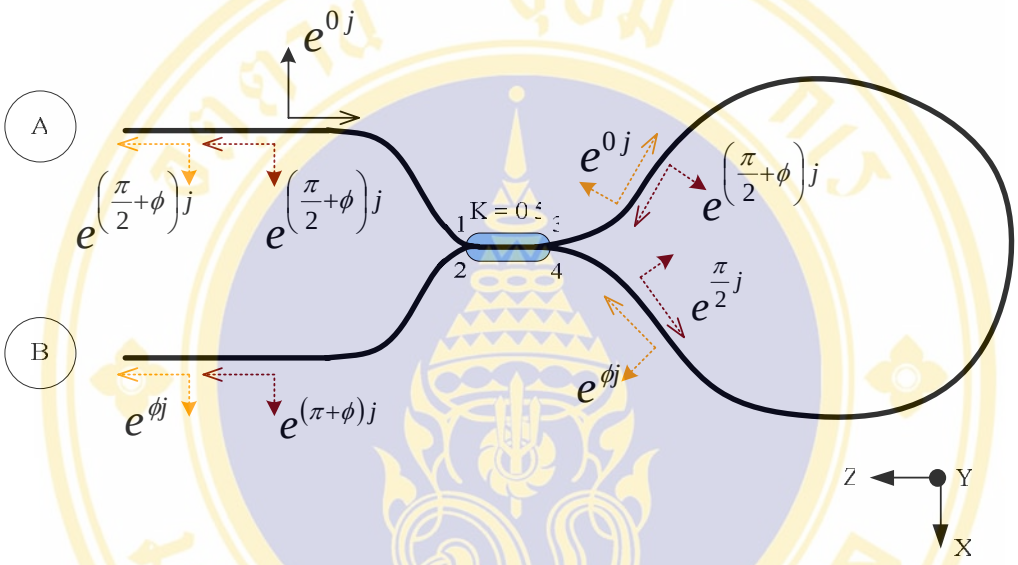

Figure 2.2 Propagation of p-polarized optical beam around the FLM when the FLM acts as a full waveplate.

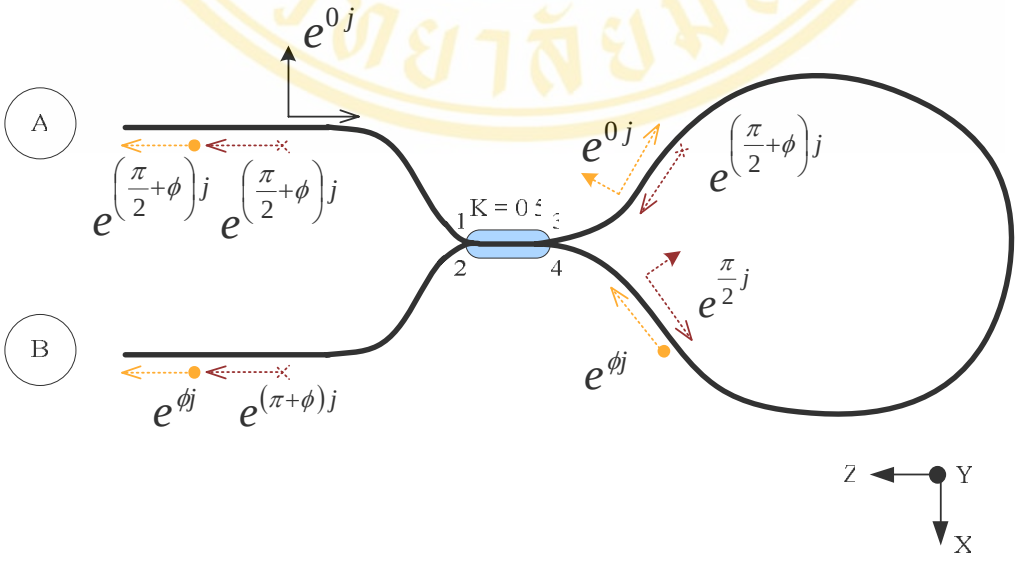

Figure 2.3 Propagation of p-polarized optical beam around the FLM when the FLM acts as a half waveplate oriented at 45° with respect to the y axis.

Copyright by Mahidol University

To switch output light from the port A to the port B, the fiber loop has to behave as a half waveplate oriented at 45° with respect to the y axis as shown in Fig. 2.3. This can be done by twisting, bending, or pressing the optical fiber inside the loop. In this case, once the clockwise optical beam from the port 3 of the 2×2 fiber-optic coupler reaches the port 4 of the 2×2 fiber-optic coupler, it is rotated by 90° with its polarization vector pointing along +y direction. Similarly, the counterclockwise optical beam from the port 4 of the 2×2 fiber-optic coupler is also rotated by 90° once it arrives at the port 3 of the 2×2 fiber-optic coupler but its polarized vector is opposite to that at the port 4. These two optical beams interfere at the 2×2 fiber-optic coupler and come out at the ports A and B. However, even though they have the same phase shift, their polarization vectors are in the opposite direction. Hence, a destructive interference occurs at the port A and there is no light here. On the other hand, the port B contains two optical beams having opposite phase and opposite polarization vector, implying that a constructive interference happens at the port B and light comes out at this port. Note that these two modes of operation of the FLM can be applied for the s-polarized optical beam as well.

From the basic operation of the FLM, the output powers at the port A and the port B can be written as [6].

$$P_A = L\left(10^{-2\gamma/10}\right)\left\{4K(1-K)\left|J\right|^2\right\}P_{in}\,, \tag{2.1}$$

and

$$P_B = L\left(10^{-2\gamma/10}\right)\left\{1-4K(1-K)\left|J\right|^2\right\}P_{in}\,, \tag{2.2}$$

where

$$\left|J\right|^2 = \left|e^{j\Delta\phi}\sin^2\theta+\cos^2\theta\right|^2. \tag{2.3}$$

Here, θ is the orientation angle of the equivalent optical phase retardation element inside the FLM, $\Delta\phi$ is the optical phase retardation inside the FLM, γ is the excess optical loss of the 2×2 fiber-optic coupler expressed in decibels, L is the optical loss of the FLM, and P_{in} is the input optical power.

Copyright by Mahidol University

2.3 Applications

Based on the basic operation of the FLM, its theory has been investigated extensively in linear and non-linear behaviors. Its transmission characteristics was also widely studied through twisting optical fiber [7-9], adjusting the polarization angle [10], rotating waveplate inside the loop [11-12], adjusting the length of the optical fiber [13], changing the coupling ratio of the 2×2 coupler [14], and combining effects of twisting optical fiber in the loop, adjusting birefringence of the loop, and controlling the length of the optical fiber [15]. In addition, temperature sensitivity of the FLM can be reduced by using a highly birefringent photonic crystal fiber in the loop [16].

Several FLM-based applications have been proposed and experimentally demonstrated. These include a wavelength-shift-free and polarization independent optical phase conjugator [17] and a fiber-optic gyroscope with dynamic range tunability and a high 23°/h rotation rate detection [18]. All fiber-based wavelength filters using FLM were built and their tunability were obtained by adjusting the birefringence inside the loop [19-20]. The FLM was also used in several fiber laser structures. For example, it acted as a variable reflector in order to continuously vary the output power of the laser [21]. In addition, it forms a non-linear amplifying loop used in a picosecond pulse laser [22]. Furthermore, when the optical fiber inside the loop is the high birefringent fiber, multiwavelength fiber lasers with wavelength spacing tunability can be achieved either by adjusting fiber length [23] or increasing the number of fiber segments [24].

The FLM structure was also used for the implementation of fiber-based sensors. These include ultrasound [25] and high electrical current [26-28] sensors suitable for remote use and multi-point detection. In addition, beat length of the optical fiber can be investigated when the test optical fiber is inserted inside the FLM [29].

In the telecommunication application the FLM structure was employed in ultrafast fiber-optic communications and signal processing systems. In this scenario, ultrafast switching was obtained by using non linear optical Kerr effect [30], deploying a quarter wave retarder and highly twisted fiber [31], and combining non reciprocal amplifier and attenuator properties inside the fiber loop [32]. A high Q

Copyright by Mahidol University

factor can also be maintained in a long haul fiber-optic communication once the non linearity of the FLM is properly designed and utilized [33].

Apart from the ultrafast switching application, a variety of FLM-based optical modules have been demonstrated, including optical logic gates [34], an optical memory [35], an optical gain equalizer [36], a wavelength multiplexer [37], a wavelength converter [38], an optical time division multiplexer [39], optical switches [40-41], and add-drop multiplexers [42-43].

Copyright by Mahidol University

CHAPTER III
FLM-BASED ARCHITECTURE

3.1 Our proposed architecture

From the basic principle of the FLM described in chapter 2, our proposed FLM-based optical phase retardation and optical transmissivity measurement structure is shown in Fig. 3.1 [44-45]. In our proposed FLM-based structure, an optical beam is fed into the IN port and it passes through a fiber-optic circulator where the optical beam is allowed to go from the left to the right hand sides. Once the optical beam comes out of the fiber-optic circulator, it then travels to a 2×2 fiber-optic coupler in which its optical power is split into K and $1-K$ parts. In this case, one optical beam travels clockwise passing through a polarization controller (PC) first and two fiber-optic collimators. Another optical beam also travels anticlockwise passing two fiber-optic collimators first and then the PC. All optical fibers are single mode optical fibers (SMFs).

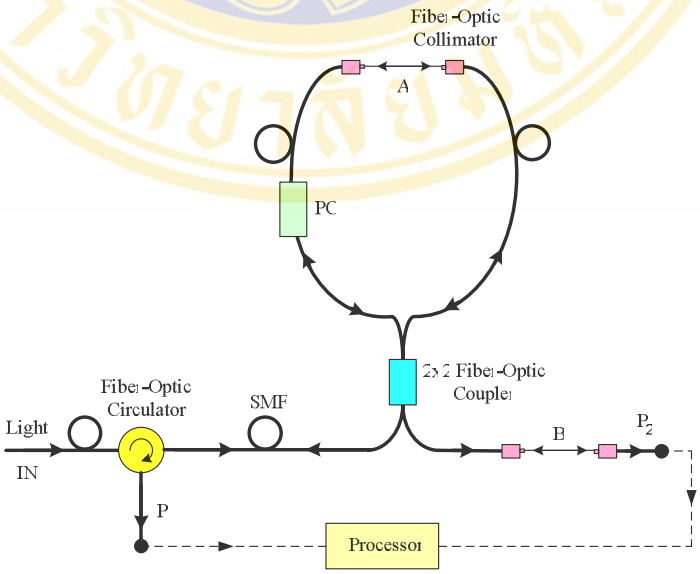

Figure 3.1 Our proposed FLM-based optical phase retardation and optical transmittivity measurement architecture.

Copyright by Mahidol University

From Eqns(2.1) and (2.2) and taking into consideration all optical losses, the optical output powers P_1 and P_2 can be expressed as.

$$P_1 = L_{1\to2}L_{2\to3}L_A\left(10^{-2\gamma/10}\right)\left\{4K(1-K)\left|J\right|^2\right\}P_{in}, \tag{3.1}$$

and

$$P_2 = L_{1\to2}L_AL_B\left(10^{-2\gamma/10}\right)\left\{1-4K(1-K)\left|J\right|^2\right\}P_{in}\,. \tag{3.2}$$

Here $L_{1\to2}$ and $L_{2\to3}$ are the optical losses of the fiber-optic circulator when the optical beam travels from the left port to the right port and from the right port to the bottom port, respectively. L_A and L_B are the coupling losses at the locations A and B, respectively.

3.1.1 Optical transmissivity measurement

To investigate the optical transmissivity of the test sample, the output optical powers of both FLM output ports need to be at the extremum level. This step ensures that the Fabry-Perot interference effect from the optical beam reflected back and forth through the FLM is suppressed. Based on Eqns(3.2) and (2.3) this can be achieved by initially adjusting the FLM to have the optical phase retardation of π so that the maximum transmitted optical power is obtained at the port 2. Then the reference sample (e.g., air and a glass slide) is inserted at the position B outside the FLM in order to measure the reference optical power $\left(P_{ref}\right)$ at the port 2. After that, the reference sample is taken out of the position B and the test sample is placed at the same location in order to measure the optical power $\left(P_{sample}\right)$. In this case, the optical transmissivity $\left(T\right)$ of the test sample can be calculated as.

$$T = P_{sample} / P_{ref}\,. \tag{3.3}$$

Eqn(3.3) is similar to Eqn(1.2), indicating that the absorption coefficient of the material can be investigated by using our proposed FLM-based structure.

Copyright by Mahidol University

3.1.2 Optical phase retardation measurement

Apart from the optical transmissivity of the test sample, we can examine its optical phase retardation as well. By measuring L_B and $L_{2\to3}$ during the initial calibration, Eqns(3.1) and (3.2) can be rewritten as.

$$P_{1n} = P_1 / L_{2\to3}, \tag{3.4}$$

and

$$P_{2n} = P_2 / L_B. \tag{3.5}$$

Since the FLM has two output ports, the normalized optical power ratios (PR) at both ports of the FLM can be expressed as.

$$PR_1 = \frac{P_{1n}}{P_{1n} + P_{2n}} = 4K(1-K)|J|^2, \tag{3.6}$$

and

$$PR_2 = \frac{P_{2n}}{P_{1n} + P_{2n}} = 1 - 4K(1-K)|J|^2. \tag{3.7}$$

From Eqn(3.6) or (3.7), it is necessary to choose an appropriate coupling coefficient K of the 2×2 fiber-optic coupler so that the desired output signal PR_1 or PR_2 is at the optimum level. For example, if we have a waveplate orientated at 45° inside the fiber loop, the optical power ratios PR_1 and PR_2 are at the lowest and highest level, respectively.

Copyright by Mahidol University

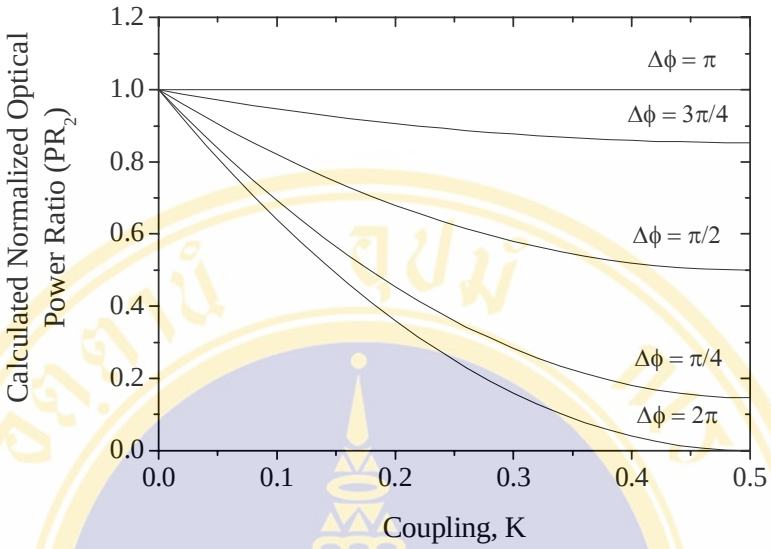

Figure 3.2 Calculated normalized optical power ratio PR_2 as a function of coupler splitting ratio and optical phase retardation.

Fig. 3.2 shows the relationship between our calculated normalized optical power ratio PR_2 and the coupling coefficient K for 5 differrent waveplates oriented at 45°. It is obvious that the optical power ratio PR_2 is dependent on the coupling coefficient K of the 2×2 fiber-optic coupler. In addition, it reaches the lowest level when the coupling coefficient K is equal to 0.5. Note that in this scenario where the waveplate is at 45° with respect to the y axis (the vertical axis), the optical power ratio PR_2 for a half waveplate (i.e., $\Delta\phi = \pi$) is always equal 1.

Once the suitable coupling coefficient K of 0.5 is chosen, we can determine the optical phase retardation value of the desired test sample (e.g., waveplate) by studying the behavior of the optical power ratio in terms of the orientation angle of the test sample. Fig. 3.3 shows our calculated normalized optical power ratio PR_2 as a function of the waveplate orientation. It points out that each waveplate has its own characteristics and therefore its optical phase retardation value can easily be analyzed.

Copyright by Mahidol University

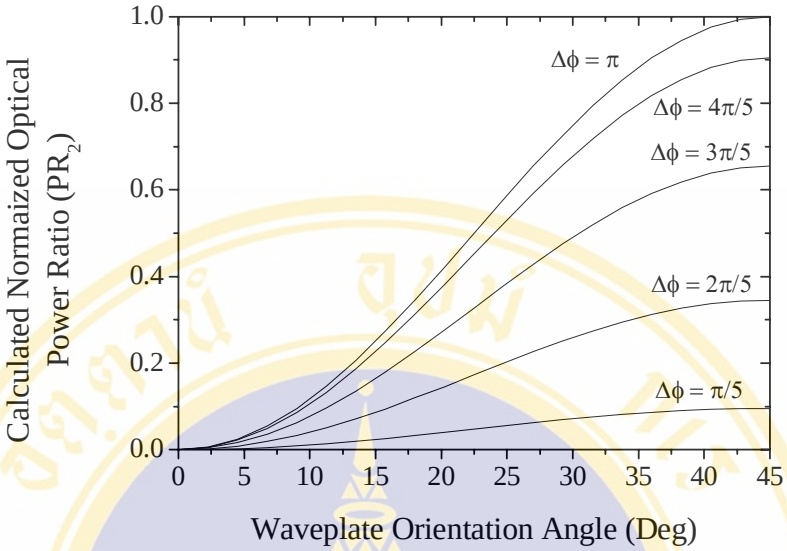

Figure 3.3 Calculated normalized optical power ratio PR_2 versus waveplate orientation angle.

With our theoretical analysis described above, the optical phase retardation of the test sample can inherently and easily be investigated by placing the test sample at the position “A”, rotating it on the plane normal to the propagation direction of the optical beam, and then measuring the optical power ratio expressed in Eqn(3.6) or Eqn(3.7). In addition to this less complicated measurement procedure, our FLM-based optical phase retardation measurement approach provides another key benefit in that all optical losses due to the insertion of the test sample at the position “A”, the optical loss inside the FLM, and the excess optical loss from the fiber-optic coupler do not affect our optical phase retardation measurement. This is unlike ref [46] where the optical loss of the test sample can affect the optical phase retardation measurement. In addition, our approach in measuring the optical phase retardation of the test sample requires a less complicated procedure compared to ref [47]. In addition, no additional component such as polarimeter and analyzer is needed. Other key features of our proposed optical transmissivity and optical phase retardation measurement structure include case of implementation, low optical loss, and low polarization dependent loss (PDL).

Copyright by Mahidol University

3.2 Experimental setup

To verify our proposed FLM-based optical transmissivity and optical phase retardation measurement concept, our experimental setup is shown in Fig. 3.4. In this case, a tunable laser diode in the C-band telecom region is connected to the fiber-optic circulator via a fiber-connectorized/angle polished contact (FC/APC) adapter. A 2×2 fiber-optic coupler having K of 50% splitting ratio is also employed. Two mechanically controlled PCs (e.g., PC1 and PC2) are inserted inside the FLM in order to easily and initially adjust the appropriate optical phase retardation of the FLM. In addition, a photodetector (PD) is used to measure both the output optical powers P_1 and P_2 and all optical fibers are SMFs.

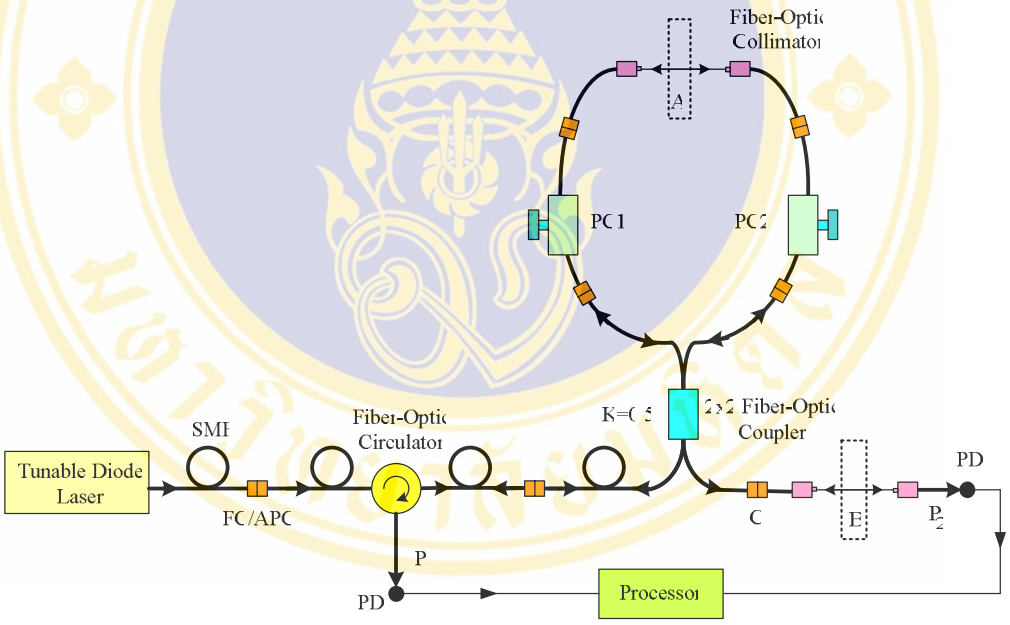

(a)

Figure 3.4 (a) Schematic illustration of our experimental setup.

Copyright by Mahidol University

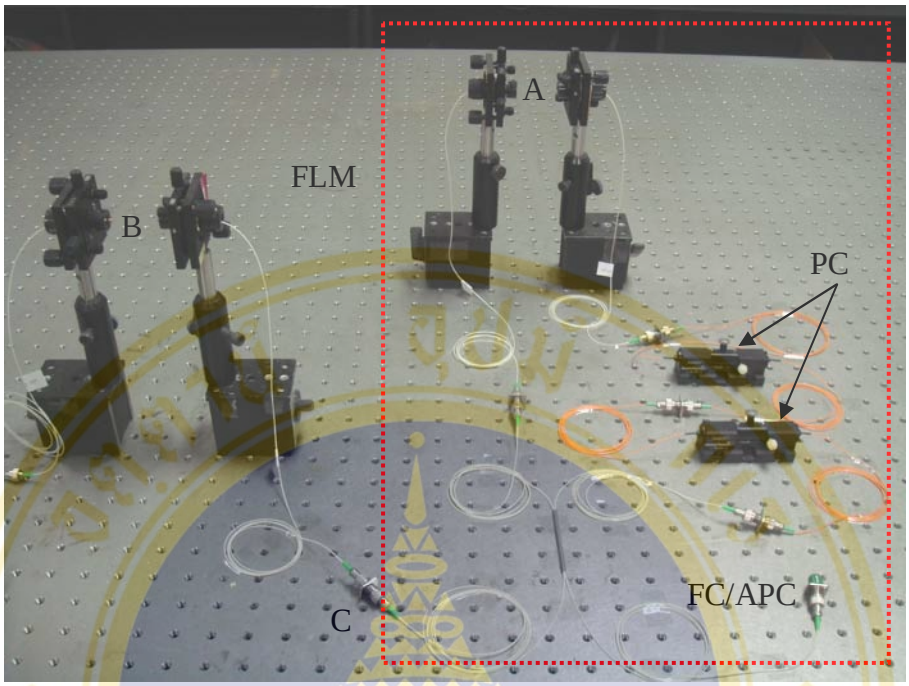

(b)

Figure 3.4 (b) photograph of our experimental setup taken at the FLM section. SMF: Single mode optical fiber. (cont.)

In our experiment, we also use three known zero-order waveplates as our test samples as shown in Fig. 3.5. During the test, each waveplate is situated on a rotational stage having 5 deg per step. The first two known zero-order waveplates are the quarter waveplate (WP1) (i.e., a 90-deg waveplate) and the half waveplate (WP2) (i.e., a 180-deg waveplate) designed to operate at a 1550-nm wavelength [48]. The last one is the HWP (WP3) designed to operate at a 632.8-nm wavelength. At 1550 nm wavelength, the WP3 has a 68.7° optical phase retardation [49].

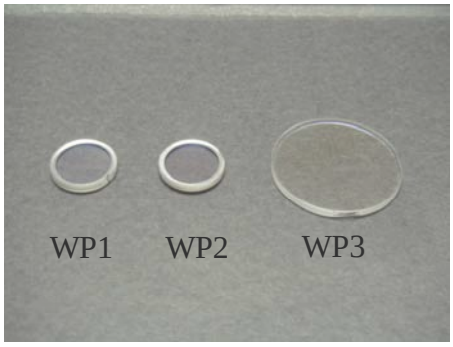

Figure 3.5 Our zero-order waveplates.

Copyright by Mahidol University

Brief information of all important optical components used in our experiment are as follows.

3.2.1 Fiber-optic circulator

A fiber-optic circulator is a device used in optical sensing systems and optical communications. Its function is to send light in forward and reverse directions. In our experiment, we use three-port fiber-optic circulator as shown in Fig. 3.6. It can transmit the incoming light from the port 1 to the port 2, and another incoming light from the port 2 to the port 3, simultaneously [50].

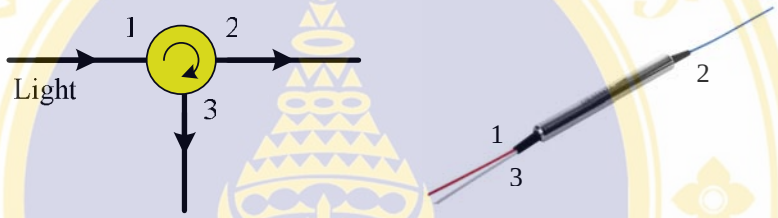

Figure 3.6 Fiber-optic circulator.

3.2.2 2×2 Fiber-optic coupler

Fiber-optic coupler is an optical device capable of branching an optical power on a single optical fiber into two optical fibers in a designated ratio. It can also combine the optical powers on two optical fibers into one. For example, with a 50:50 2×2 fiber-optic coupler shown in Fig. 3.7, the input optical power is equally divided among the two output ports [51].

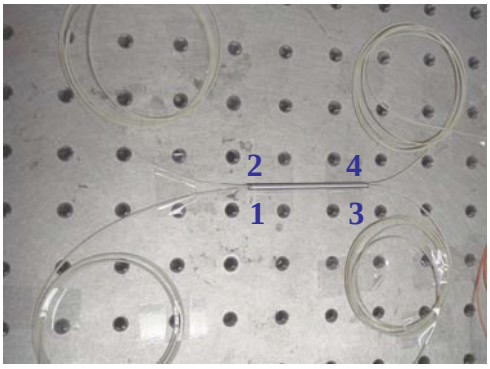

Figure 3.7 2×2 Fiber-optic coupler.

Copyright by Mahidol University

3.2.3 Fiber-optic collimator

A typical fiber-optic collimator consists of the SMF and the gradient-index (GRIN) lens as shown in Fig. 3.8. It can focus the incoming optical beam into the SMF or collimate the optical beam emerging from the SMF. It is widely used in the fiber-optic components such as fiber-optic switches and fiber-optic attenuators.

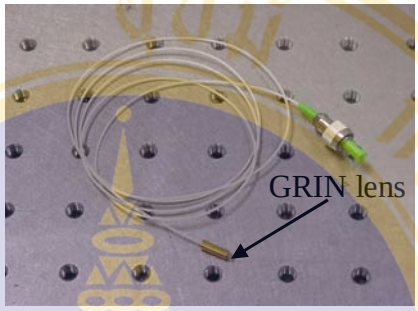

Figure 3.8 Fiber-optic collimator.

3.2.4 Polarization controller (PC)

A polarization controller consists of only a fiber optic cable with two open terminals as shown in Fig. 3.9. The center portion of the fiber strand is sandwiched in the fiber squeezer. Turning the knob on the fiber squeezer clockwise will apply pressure to the fiber center portion.

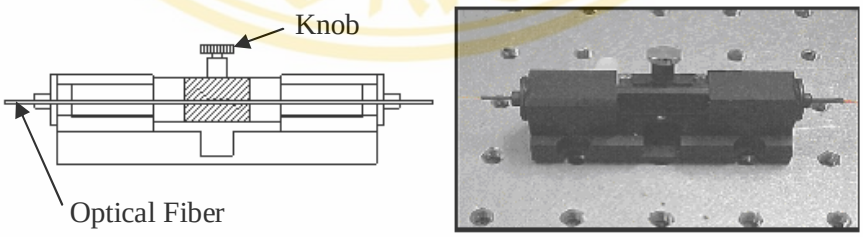

Figure 3.9 Polarization controller.

Copyright by Mahidol University

With applied pressure as shown in Fig. 3.10, the fiber center portion acts as a birefringent waveplate and the optical phase retardation can be written as [52]

$$\Delta\phi = \frac{2\pi L}{\lambda}\left(n_{\perp} - n_{//}\right). \tag{3.8}$$

Here, L is the length of the optical fiber, λ is the operating wavelength, $n_{\perp}$ is the refractive index of the ordinary ray, and $n_{//}$ is the refractive index of the extraordinary ray.

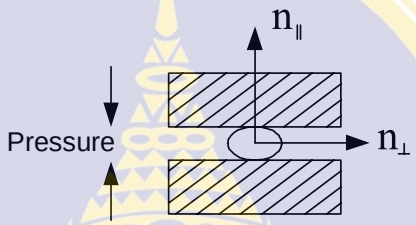

Figure 3.10 Squeezing fiber optic.

Copyright by Mahidol University

CHAPTER IV
RESULTS AND DISCUSSION

4.1 Optical isolation study

Before we investigate the optical transmissivity and the optical phase retardation of the test sample, we have to make sure that there is less amount of the optical beam reflected back and forth through the FLM. This can be determined by looking at the optical isolation of the system. The optical isolation is defined as the ratio of the measured optical power at the desired port to the measured optical power at the unwanted port. In our experiment, by adjusting the two PCs to get the maximum optical power at the port 2 for only 1550 nm wavelength optical beam, a measured optical isolation is 33.45 dB as shown in Fig. 4.1. As the operating wavelength is out of the desired wavelength, the measured optical isolation decreases over a 20-nm wavelength band with a maximum change of 2.24 dB at the 1560 nm wavelength.

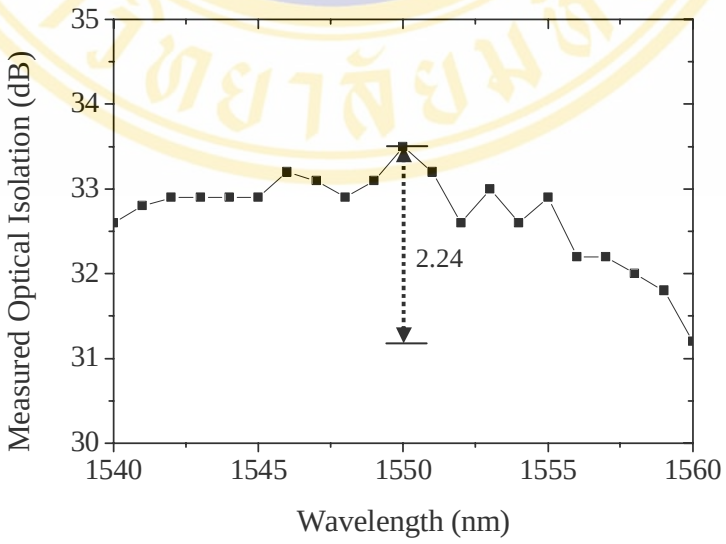

Figure 4.1 Measured optical isolation at the port P_2 when the FLM is set to operate only at 1550 nm wavelength.

Copyright by Mahidol University

This 2.24-dB maximum fluctuation in optical isolation can also be reduced by adjusting the two PCs to have the best optical isolation for any desired wavelength at a time. In this case, the measured maximum optical isolation is 33.1±1.9 dB over a 20 nm wavelength band as shown in Fig 4.2. In other words, the ratio of P_2 and P_1 is about 2089 which is high enough to investigate the optical transmittivity and the optical phase retardation of the test sample in this wavelength band.

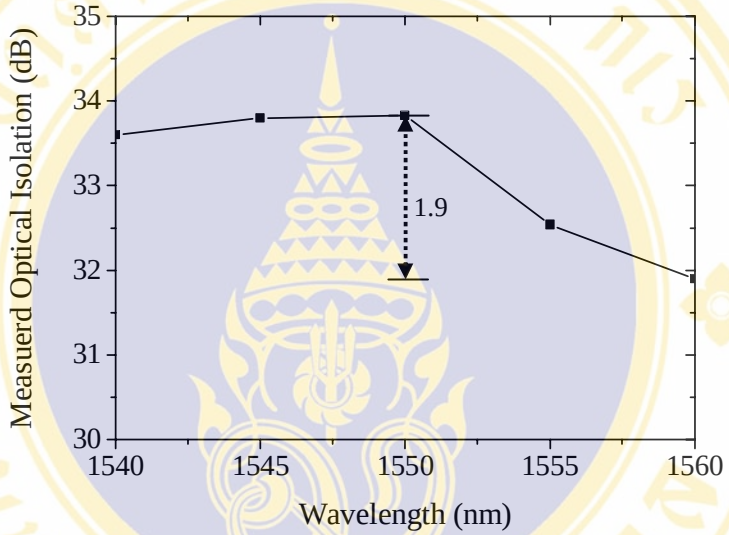

Figure 4.2 Measured optical isolation at the port P_2 when the FLM is optimized to operate at any desired wavelength.

4.2 Optical loss study

Another important system issue is the optical loss. It is the ratio of the output optical power at the port 2 and the input optical power in front of the fiber-optic circulator. A measured optical loss of 2.47 dB is determined and it is limited by eight FC/APC adapters (0.2 dB), a one-way trip through the fiber-optic circulator (i.e., $-10LogL_{1\to 2}$ = 0.5 dB), two PCs (0.13 dB), and free-space coupling efficiency at the locations A and B (1.64 dB).

Copyright by Mahidol University

4.3 Polarization dependent loss study

PDL is a measure of the peak-to peak difference in transmission of an optical component or system with respect to all possible states of polarization. It is the ratio of the maximum and the minimum optical output powers with respect to all polarization states. PDL in decibels is defined as.

$$PDL = 10 \times \log\left(\frac{P_{\max}}{P_{\min}}\right). \tag{5.2}$$

In this case, by scrambling the state of polarization of the input light in front of the fiber-optic circulator, a measured PDL of 0.38 dB is obtained.

4.4 Optical transmissivity study

For our optical transmissivity measurement, we initially adjust the two PCs inside the FLM such that we have a maximum optical output power at the port 2. We also make sure that a high optical isolation of > 31 dB is still obtained. Fig. 4.3-4.5 shows our measured optical transmissivity values for all three test samples from both measurement systems. Note that our reference sample is air.

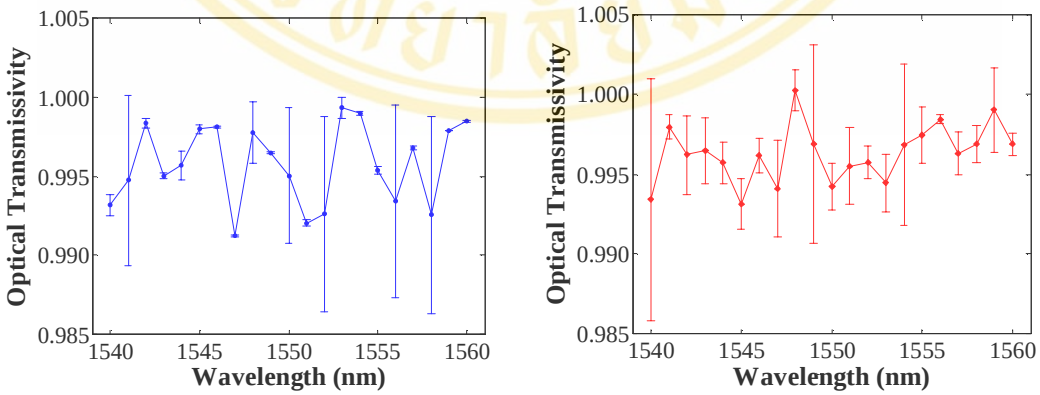

(a) (b)

Figure 4.3 Measured optical transmissivity versus operating wavelength for WP1 in (a) an optical spectrometer and (b) our FLM-based structures.

Copyright by Mahidol University

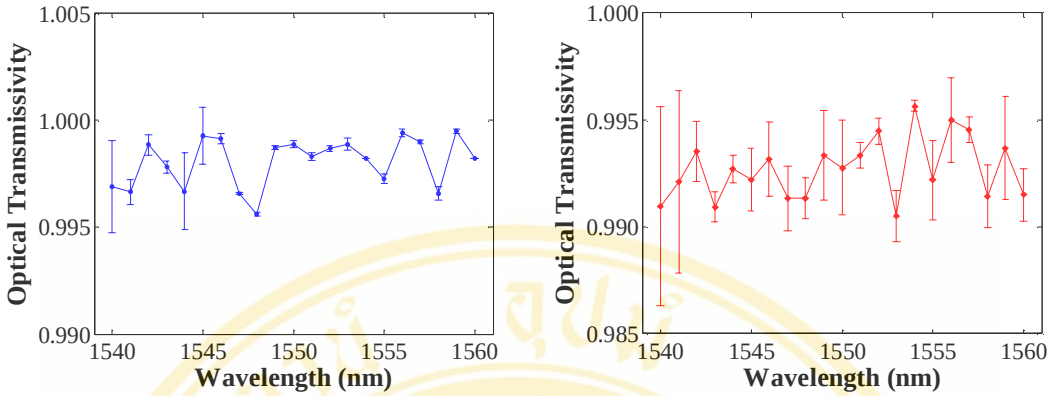

(a) (b)

Figure 4.4 Measured optical transmissivity versus operating wavelength for WP2 in (a) an optical spectrometer and (b) our FLM-based structures.

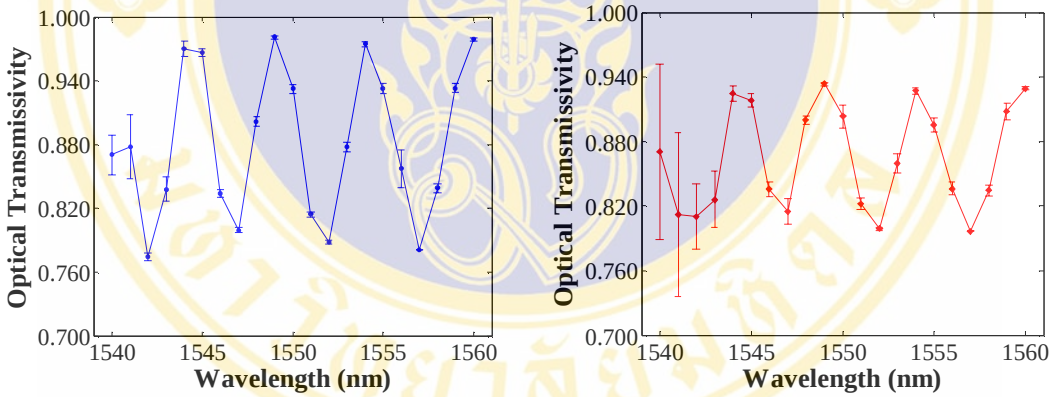

(a) (b)

Figure 4.5 Measured optical transmissivity versus operating wavelength for WP3 in (a) an optical spectrometer and (b) our FLM-based structures.

We also compare our experimental results obtained from our proposed FLM-based approach with a typical optical spectrometer. In our experiment, the optical spectrometer is formed by just connecting the tunable laser directly at the position C (see Fig. 3.4 in Chapter 3). It can be observed that the optical transmissivity measurements for the WP1 and WP2 have small fluctuation of < 0.76% and < 0.47% from both architectures, respectively. In addition, these two measurement systems

Copyright by Mahidol University

provide similar optical transmissivity measurement for the WP1 and WP2 with a < 0.84% difference, limited by a < 3% accuracy of the PD and the photodetection noise in the system. For the WP3, a 6.6% variation of the measured optical transmissivities versus test wavelength is observed which is much higher compared to the previous two samples. There is also a higher < 8% fluctuation in optical transmissivity measurement for the WP3. This is because the WP3 is optimally designed to operate only at the 632.8 nm wavelength and therefore the reflection loss from its front and back surfaces induces the Fabry-Perot interference effect. Hence, based on our optical transmissivity study, our FLM-based approach can function as an optical spectrometer.

4.5 Optical phase retardation study

For our optical phase retardation analysis of the test sample, we choose to initially adjust the two PCs inside the FLM so that we have a maximum reflected optical power at the port 1. Then we insert our test sample at the position A and rotate it from 0° to 45° in a step of 5°.

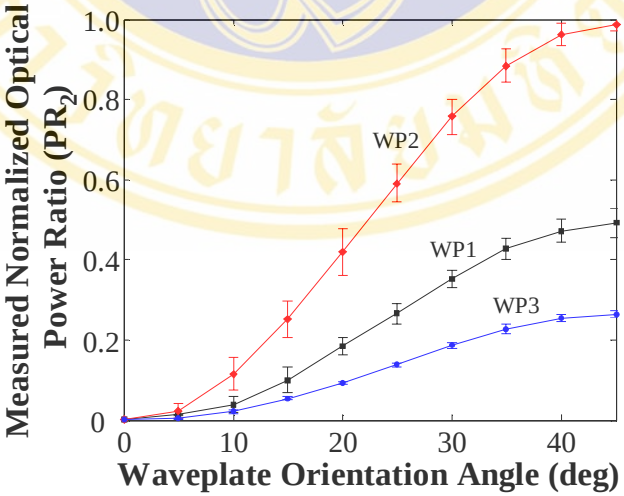

Figure 4.6 Measured normalized optical power ratio versus waveplate orientation angle for (a) WP1, (b) WP2, and (c) WP3: circle symbol and line are from our experimental and theoretical results, respectively.

Copyright by Mahidol University

Fig. 4.6 shows our measured normalized optical power ratio versus the rotation angle for all three waveplates. There are also fluctuations of <3.6%, < 5.8%, and < 1.2% in measuring the normalized optical power ratio PR_2 for the WP1, WP2, and WP3, respectively. It can be noticed that a waveplate with a higher optical phase retardation value has a larger PR_2 fluctuation. This is because of the use of a larger-step rotational stage that a small rotational movement leads to a higher fluctuation in measuring optical powers at the port 1 and port 2. By using eqn(3.7) with measured $L_{2\to3}$ = 0.88 and L_B = 0.80, the optical phase retardation values for the WP1, WP2, and WP3 are 89°, 179°, and 67.7° are determined, respectively. There is also a 1° difference between our experimental results and the expected values and it is limited by the resolution of our rotational stage. By varying the test wavelength, optical phase retardation values of the three test samples with a small error of < 1° are achieved as shown in Fig. 4.7, confirming that these three test waveplates are indeed zero-order waveplates. Hence, this experimental result confirms that our FLM-based configuration can be used to analyze the optical phase retardation of the test sample as well.

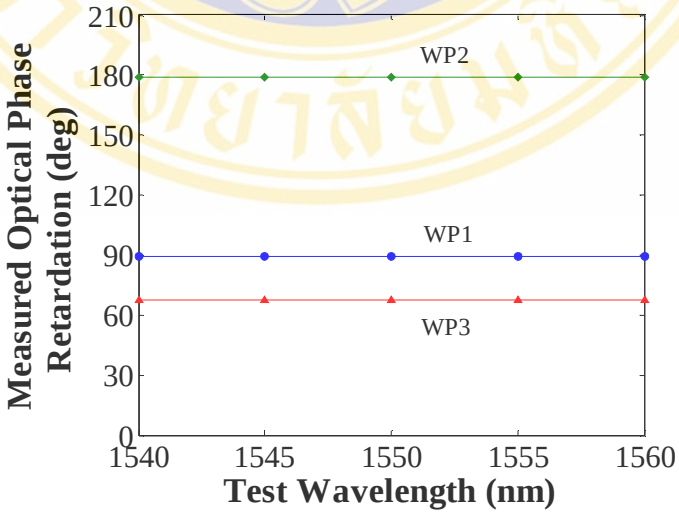

Figure 4.7 Measured optical phase retardation versus test wavelength for (a) WP1, WP2 and WP3.

Copyright by Mahidol University

CHAPTER V
CONCLUSIONS

We have proposed and experimentally demonstrated an FLM-based optical phase retardation and optical transmissivity measurement structure. Our proposed FLM-based measurement system is all-fiber based and it simply consists of a fiber-optic coupler, a polarization controller, and a fiber-optic circulator. Our key idea comes from the use of the inherent FLM operation, allowing the flexibility to control the optical output powers to the extremum level via varying optical phase retardation inside the FLM. Without the test sample, our proposed FLM-based optical phase retardation and optical transmissivity measurement system offers a very high measured optical isolation of 33.1 dB, a 2.47 optical loss, and a PDL of 0.38 dB.

We have also presented an experimental analysis of the optical transmissivity in the FLM. Our experimental result from the FLM-based structure corresponds to the result obtained from a non-FLM system. In addition, there is a very small < 0.84% fluctuation in our measured optical transmissivity values for both cases, limited by a < 3% accuracy of our PD used in our experiment.

In addition, we have presented a very simple technique in eliminating the affect of the optical losses from the test sample and the FLM itself in order to measure the optical phase retardation of the test sample. Our propose technique is to analyze the ratio of the optical powers from both the reflection and transmission ports of the FLM. Our experimental demonstration using three known zero-order waveplates as our test samples shows promising results associated with the defined phase retardation values having a small error of < 1° over a 20 nm wavelength band. Our experiment with wavelength tunability provided by the laser source also confirms that these three waveplates are designed as zero-order waveplates.

We believe that the proposed architecture will play an important role in the development of a more advanced but yet simple optical sensing system. In the future,

Copyright by Mahidol University

we plan to test the performance of our FLM-based optical phase retardation and optical transmissivity measurement structure with other samples as well as to optimize its functionality.

Copyright by Mahidol University

REFERENCES

1. B. Henderson, "Optical spectrometers," Chap. 20 in *Handbook of Optics*, Vol. II, M. Bass, E. W. Van Stryland, D. R. Williams, and W. L. Wolfe, Eds., McGraw-Hill, pp. 20.1-20.3, 1995.
2. B. A. Saleh and M. C. Teich, *Fundamentals of Photonics*, John Wiley & Sons, 1991.
3. R. A. Chipman, "Polarimetry," Chap. 22 in *Handbook of Optics*, Vol. II, M. Bass, E. W. Van Stryland, D. R. Williams, and W. L. Wolfe, Eds., McGraw-Hill, pp. 22.1-22.20, 1995.
4. H.- F. Chang, C. Chou, H.- K. Teng, H.- T. Wu, and H.- F. Yau, "The use of polarization modulation and amplitude-sensitive optical heterodyne interferometry for linear birefringence parameters measurement," *Optics Communications*, Vol. 258, pp. 420-426, 2006.
5. K. Ichimoto, K. Shinoda, T. Yamamoto, and J. Kiyohara, "Photopolarimetric measurement system of Mueller Matrix with dual rotating waveplates," *Publication of the National Astronomical Observatory of Japan*, Vol. 9, No. 1-2, pp. 11–19, 2006.
6. D. B. Mortimore, "Fiber loop reflectors," *Journal of Lightwave Technology*, Vol. 6, pp. 1217-1224, 1988.
7. H. H. Cerecedo-Nunez, E. A. Kuzin, J. J. Sanchez-Mondragon, and E. Molina, "A simplified technique for the adjustment of a birefringent optical fiber Sagnac interferometer," *Part of the 18th Congress of the international Commission for Optics*, Vol. 3749, pp. 709-710, August 1999.
8. J. M. Estudillo-Ayala, J. Ruiz-Pinales, R. Rojas-Laguna, J. A. Andrade-Lucio, O. G. Ibarra-Monzano, E. Alvarado-Mendez, M. Torres-Cisneros, B. Ibarra-Escamilla, and E. A. Kuzin, "Analysis of Sagnac interferometer with low-birefringence twisted fiber," *Optics and Lasers in Engineering*, Vol. 39, pp. 635-643, 2003.

Copyright by Mahidol University

9. E. A. Kuzin, H. C. Nunez, and N. Korneev, “Alignment of a birefringent fiber sagnac interferometer by fiber twist,” *Optics Communications*, Vol. 160, pp. 37-41, 1999.
10. C. A. Merchant and A. L. Steele, “A tunable nonlinear optical loop mirror with feedback using linear highly birefringent fiber in the loop,” *Optics Communications*, Vol. 258, pp. 288-294, 2006.
11. B. Ibarra-Escamilla, E. A. Kuzin, O. Pottiez, J. W. Haus, F. Gutierrez-Zainos, R. Grajales-Coutino, and P. Zaca-Moran, “Fiber optical loop mirror with a symmetrical coupler and a quarter-wave retarder plate in the loop,” *Optics Communications*, Vol. 242, pp. 191-197, 2004.
12. O. Pottiez, E. A. Kurin, B. Ibarra-Escamilla, an F. M. Martinez, “Easily tunable nonlinear optical loop mirror including low-birefringence, highly twistd fibre with invariant output polarization,” *Optics Communications*, Vol. 229, pp. 147-159, 2004.
13. E. A. Kuzin, J. A. Andrade-Lucio, B. I. Ecamilla, R. Rojas-Laguna, and J. Anchez-Mondragon, “Nonlinear optical loop mirror using the nonlinear polarization rotation effect,” *Optics Communications*, Vol. 144, pp. 60-64, 1997.
14. D. D. Shah, J. Ravikanth, and R. Vijya, “Optimization of peak transmittivity in a non-linear fiber loop mirror-an accurate analysis,” *Optics Communications*, Vol. 197, pp. 301-308, 2001.
15. E. A. Kuzin, B. I. Ecamilla, R. R. Laguna, and J. S. Mondragon, “Nonlinear optical loop mirror with low birefringence twisted fiber in the loop,” *Optics Communications*, Vol. 149, pp. 73-76, 1998.
16. C.- L. Zhao, X. Yang, C. Lu, W. Jin, and M. S. Demokan, “Temperature-insensitive interferometer using a highly birefringent photonic cystal fiber loop mirror,” *IEEE Photonics Technology Letters*, Vol. 16, No. 11, pp. 2535-2537, November 2004.
17. H. C. Lim, F. Futami, and K. Kikuchi, “Polarization-independent, wavelength-shift-free optical phase conjugator using a nonlinear fiber Sagnac interferometer,” *IEEE Photonics Technology Letters*, Vol. 11, No. 5, pp. 578-580, May 1999.

Copyright by Mahidol University

18. C.- Y. Liaw, Y. Hou, and Y.- L. Lam, "Characterization of an open-loop interferometric fiber-optic gyroscope with the Sagnac coil closed by an erbium-doped fiber amplifier," *Journal of Lightwave Technology*, Vol. 16, No. 12, pp. 2385-2392, December 1988.
19. Y. Han, Q. Li, X. Liu, and B. Zhou, "Architecture of high-order all-fiber birefringent filters by the use of the Sagnac interferometer," *IEEE Photonics Technology Letters*, Vol. 11, No. 1, pp. 90-92, January 1999.
20. Y. W. Lee, K. J. Han, B. Lee, and J. Jung, "Polarization-independent all-fiber multiwavelength-switchable filter based on a polarization-diversity loop configuration," *Optics Express*, Vol. 11, No. 25, pp. 3359-3364, December 2003.
21. C. A. Millar, I. D. Miller, D. B. Mortimore, B. J. Ainslie, and P. Urquhart, "Fibre laser with adjustable fibre reflector for wavelength tuning and variable output coupling," *IEEE Proceedings*, Vol. 135, No. 4, pp. 303-309, August 1988.
22. N. J. Traynor, A. B. Grudinin, V. Pruneri, A. A. Sysoliatin, and V. A. Semenov, "Tunable source of picosecond pulses around 1550 nm for all-optical processing," *Optics Communications*, Vol. 139, pp. 237-240, 1997.
23. X. P. Dong, S. Li, K. S. Chiang, M. N. Ng, and B. C. B. Chu, "Multiwavelength erbium-doped fibre laser based on a high-birefringence fibre loop mirror," *Electronics Letters*, Vol. 36, No. 19, pp. 1609-1610, September 2000.
24. L. R. Chen, "Tunable multiwavelength fiber ring lasers using a programmable high-birefringence fiber loop mirror," *IEEE Photonics Technology Letters*, Vol. 16, No. 2, pp. 410-412, Febuary 2004.
25. T. S. Jang, S. S. Lee, and Y. G. Kim, "Surface-bonded fiber optic Sagnac sensors for ultrasound detection," *Ultrasonic*, Vol. 42, pp. 837-841, 2004.
26. M. F. Chan, G. Chen, M. S. Demokan, and H. Y. Tam, "Optimal sensing of current based on extrinsic Sagnac interferometer configuration," *Optics and Lasers in Engineering*, Vol. 30, pp. 17-24, 1998.

Copyright by Mahidol University

27. H. Lin, and S. C. Huang, “Fiber-optics multiplexed interferometric current sensors,” *Sensors and Actuators A*, Vol. 121, pp. 333-338, 2005.
28. J. Blake, P. Tantaswadi, and R. T. de Carvalho, “In-line Sagnac interferometer current sensor,” *IEEE Transactions on Power Delivery*, Vol. 11, No. 1, pp. 116-121, January 1996.
29. B. Ibrra-Escamilla, E. A. Kuzin, F. Gutierrez-Ainos, R. Tellez-Garcia, J. W. Haus, R. Rojas-Laguna, and J. M. Estudillo-Ayala, “Measurement of beat length in short low-birefringence fiber using the fiber optical loop mirror,” *Optics Communications*, Vol. 217, pp. 211-219, 2003.
30. M. Jinno, “Nonlinear Sagnac interferometer switch and its applications,” *IEEE Journal of Quantum Electronics*, Vol. 28, No. 4, pp. 875-882, April 1992.
31. O. Pottiez, B. Ibarra-Escamilla, and E. A. Kuzin, “Demonstration of sharp switching from a power-symmetric NOLM and a polarizer,” *Optics Communications*, Vol. 271, pp. 543-550, 2007.
32. A. W. O’Neill, and R. P. Webb, “All-optical loop mirror switch employing an asymmetric amplifier/attenuator combination,” *Electronics Letters*, Vol. 26, No. 24, pp. 2008-2009, 1990.
33. A. Labruyere, and P. T. Dinda, “Analytical design of nonlinear optical loop mirror for fiber-optic communication systems,” *Optics Communications*, Vol. 266, pp. 676-680, 2006.
34. A. Huang, N. Whitaker, M. Auramopoulos, P. French, M. Hough, and I. Chuang, “Sagnac fiber logic gates and their possible applications: a system perspective,” *Applied Optics*, Vol. 33, No. 20, pp. 6254-6267, 1994.
35. Y. Chai, J. H. Chen, F. S. Choa, J. P. Zhang, J. Y. Fan, and W. Lin, “Scalable and modularized optical random-access memories for optical packet-switching networks,” *CLEO’98*, pp. 397, 1998.
36. J.- X. Cai, K.- M. Feng, X. P. Chen, and A. E. Willner, “Equalization of nonuniform EDFA gain using a fiber-loop mirror,” *IEEE Photonics Technology Letters*, Vol. 9, No. 7, pp. 316-318, 1997.

Copyright by Mahidol University

37. X. Fang and R. O. Claus, "Polarization-independent all-fiber wavelength-division multiplexer based on a Sagnac interferometer," *Optics Letters*, Vol. 20, No. 20, pp. 2146-2148, 1995.

38. E. A. Swanson and J. D. Moores, "A fiber frequency shifter with broad bandwidth, high conversion efficiency, pump and pump ASE cancellation, and rapid tunability for WDM optical networks," *IEEE Photonics Technology Letters*, Vol. 6, No. 11, pp. 1341-1343, 1994.

39. I. Glesk, J. P. Sokoloff, and P. R. Prucnal, "Demonstration of all-optical demultiplexing of TDM data at 250 Gbits/s," *Electronics Letters*, Vol. 30, No. 4, pp. 339-341, 1994.

40. O. A. Pattison, P. N. Kean, W. Forysiak, I. Bennion, and N. J. Doran, "Bandpass switching in a nonlinear-optical loop mirror," *Optics Letters*, Vol. 20, No. 4, pp. 362-364, 1995.

41. R. J. Manning, A. E. Kelly, A. J. Poustie, and K. J. Blow, "Wavelength dependence of switching contrast ratio of semiconductor optical amplifier-based nonlinear loop mirror," *Electronics Letters*, Vol. 34, No. 9, pp. 916-918, 1998.

42. J. W. Lou, T. J. Xia, Y. Liang, Y. H. Kao, O. Boyraz, K. H. Ahu, and M. N. Islam, "All-optical TDM add/drop multiplexer demonstration with 100-Gbits/s words," *CLEO'98*, pp. 3-4, 1998.

43. S. Sumriddetchkajorn and N. A. Riza, "Fiber-connectorized multiwavelength 2×2 switch structure using a fiber loop mirror," *Optics Communications*, Vol. 175, pp. 89-95, 2000.

44. S. Sumriddetchkajorn, "Methods for determining the optical absorption coefficient and the optical phase retardation of the material by using a fiber loop mirror," *Thai Patent Application*, 0701001916, April 2007.

45. K. Katanyukunanon, S. Sumriddetchkajorn, and T. Srikhirin, "A study of optical phase retardation and absorption measurement by using a fiber loop mirror architecture," *Proceedings of the 2007 International Conference on Electrical Engineering/Electronics, Computer, Telecommunications, and Information Technology*, Chiang Rai, Thailand, May 2007.

Copyright by Mahidol University

46. I. Golub and E. Simuva, “π–shifted Sagnac interferometer for characterization of femtosecond first- and second-order polarization mode dispersion,” *Optics Letters*, Vol. 27, No. 19, pp. 1681-1683, 2002.
47. E. Simuva and I. Golub, “Phase-stepping an all-fiber Sagnac loop for full characterization of femtosecond PMD,” *IEEE Photonics Technology Letters*, Vol. 15, No. 7, pp. 960-962, 2003.
48. Thorlabs, Inc., 435 Route 206, North Newton, New Jercy, USA, 07860.
49. L. Xanthe, Private Communication, CASIX Inc., P.O. Box 1103, Fuzhou, Fujian 350014, China, February 2007.
50. http://www.afwtechnologyom.au, July 3, 2007.
51. http://optical-components.globalspec.com/ProductFinder, August 3, 2007.
52. General Photonics Corporation, 13766 Arapahoe Place, Chino, California 19710 USA.

Copyright by Mahidol University

BIOGRAPHY

NAME	Ms. Kanitha Katanyukunanon
DATE OF BIRTH	Nov 18, 1982
PLACE OF BIRTH	Phrae, Thailand
INSTITUTIONS ATTENDED	Thammasat University, 2001-2004: Bachelor of Science (Physics) Mahidol University, 2005-2007: Master of Science (Physics)
RESEARCH GRANT	Recipient of scholarship from the Thailand Graduate Institute of Science and Technology, 2005-2007
HOME ADDRESS	95/1 M.7 Yantarakitkoson Road, T. Rongkwang, A. Rongkwang Phrae 54140 Thailand Tel. 08-1205-4757
E-MAIL	bleamberry@hotmail.com

Copyright by Mahidol University